SECOND EUROPEAN CONFERENCE ON EARTHQUAKE ENGINEERING
AND SEISMOLOGY, ISTANBUL AUG. 25-29, 2014

FRAMEWORK FOR DEVELOPING FRAGILITY RELATIONS OF HIGH-RISE RC WALL BUILDINGS BASED ON VERIFIED MODELLING APPROACH

Wael ALWAELI[1], Aman MWAFY[2], Kypros PILAKOUTAS[3], Maurizio GUADAGNINI[4]

ABSTRACT

This paper presents a framework and exemplar application for the development of reliable analytical seismic fragility relations (ASFRs) for code-compliant, reinforced-concrete (RC) high-rise wall structures. A multi-level verification scheme is applied to investigate different approaches and parameters to be adopted in nonlinear analytical modelling of RC high-rise buildings with slender shear walls and cores. The verification scheme includes the modelling of a seven-story wall building slice tested at full scale on the Large High-Performance Outdoor Shake Table (LHPOST) at the University of California, San Diego (UCSD). In the proposed framework, incremental dynamic analyses (IDAs) method with improved intensity measure (IM) is used to develop the fragility relations for RC high-rise wall structures based on defined performance limit states (PLSs). For a given seismic intensity level, the probability of exceedance for each PLS is estimated and results can be integrated with conventional probabilistic seismic hazard analysis (PSHA) to estimate the seismic vulnerability of these structures. The framework is illustrated by developing ASFRs for a sample structure of 30-story RC wall building located in the Emirate of Dubai (UAE); a region that is taken as case study in the current work. The paper reveals the advantages of implementing fibre-based 4-noded wall/shell element modelling approach to account for 3D effects of deformation compatibility between lateral and gravity-force-resisting systems. It also underlines the sensitivity of ASFRs to the structural damage measure (DM) values used to define the PLSs.

1. INTRODUCTION AND METHODOLOGY

Whilst the number of high-rise buildings and skyscrapers with different lateral-force-resisting systems that are vulnerable to multiple earthquake scenarios is increasing worldwide, there have been only limited attempts to establish refined ASFRs for RC high-rise wall structures (Ji et al, 2009; Mwafy 2010) based on verified nonlinear modelling approaches. Based on modern seismic codes, earthquake-resistant buildings are designed and detailed to respond inelasticly under the design-based and maximum considered earthquakes. Hence, a reliable nonlinear modelling methodology of building response is essential in assessing the vulnerability of such structures. Given that published experiment tests data of RC structural wall systems subjected to cycling load are very limited, as most of the tests conducted so far are on isolated wall elements, it is essential to verify the nonlinear modelling techniques and parameters against full-scale, shake-table experimentally tested RC wall structures.

[1] Corresponding Author, The University of Sheffield, UK, wael.mahdi@sheffield.ac.uk
[2] Associate Professor, United Arab Emirates University, UAE, amanmwafy@uaeu.ac.ae
[3] Professor, The University of Sheffield, UK, k.pilakoutas@sheffield.ac.uk
[4] Senior Lecturer, The University of Sheffield, UK, m.guadagnini@sheffield.ac.uk

Nonlinear response history analysis (NRHA) stands as the most exact tool currently available for predicting building response at different levels of ground motion intensity. In NRHA, the accuracy of the nonlinear model is measured by its ability to capture significant modes of deformation and deterioration in the analysed structure from the onset of damage to collapse. Various aspects of nonlinear modelling, such as element discretization, material force-deformation relationships, and assumptions on modelling of viscous damping are essential in defining the level of accuracy a model can have in predicting the seismic global and local response of the structure.

The aim of the present study is to present a complete framework to derive reliable ASFRs for code-compliant RC high-rise wall buildings based on verified nonlinear modelling techniques and parameters. As a key step towards constructing the said framework, a multi-level modelling assessment is conducted by investigating two macroscopic modelling approaches: (i) fibre-based 2-noded beam-column line element (also called wide-column element); and (ii) fibre-based 4-noded wall/shell element. ZEUS-NL (Elnashai et al., 2012) is utilized to implement the former modelling approach, while PERFORM-3D (CSI, 2011) is chosen to investigate the latter. The verification process is conducted on three levels: (i) the modelling of a 5-story pier; (ii) the modelling of a 10-story core; and (iii) the simulation of the nonlinear dynamic response of a full-scale seven-story wall building slice using three different modelling techniques. This building slice was tested under base excitations representing four earthquake records of increasing intensities on the LHPOST at UCSD (Panagiotou et al., 2007). Due to space limitations, only sample results of the third level of the modelling verification scheme are presented hereafter.

The nonlinear modelling approach and key modelling parameters were decided on the basis of the conducted modelling verification scheme. The additional steps in the proposed framework are illustrated in the following through a sample structure of a 30-story RC wall building located in Dubai (UAE); a region that is taken as case study in the current work. The sample building is designed and detailed according to the codes and standards adopted in the studied region. To perform IDAs, a series of NRHAs are conducted under a multiply scaled suite of forty real ground motion records selected to represent two different earthquake scenarios applicable to the studied region. An improved IM that accounts for structure softening and effects of higher modes is proposed, while maximum, overall stories, peak interstory drift (ISD) ratio are chosen as structural DM. Three PLSs are defined to be represented in the fragility relations: (i) Immediate Occupancy “IO”; (ii) Life Safety “LS”; and (iii) Collapse Prevention “CP”. Proper techniques are implemented to estimate the probability distribution of the structural demand given the seismic intensity.

2. VERIFICATION OF ANALYTICAL MODELS: UCSD SHAKE TABLE TEST

To validate the nonlinear modelling approaches and key modelling parameters discussed in the preceding sections, three analytical models are developed and their NRHA results are compared with the experimental data of a 7-story full-scale RC building slice: (i) a 2D preliminary model developed using ZEUS-NL **“Z-MODEL”**; (ii) an improved 2D version of Z-Model **“IZ-MODEL”**; and (iii) a 3D model developed using PERFORM-3D **“P-MODEL”**. The test program was performed on the LHPOST at UCSD as part of the George E. Brown Jr. Network for Earthquake Engineering Simulation (NEES) program. The test was conducted in two phases; Phase I: Rectangular Wall and Phase II: T-Wall. Test results from Phase I are selected for the verification program, including ISDs, story displacements, story shears, story moments, period elongation and local strains. Detailed information about the test program and Phase-I test results are available in Panagiotou et al., 2007.

2.1 DESCRIPTION OF THE TEST STRUCTURE

The test structure consisted of a 3D slice of a 7-story prototype residential load bearing wall building located in Los Angeles, California (Fig. 1). In Phase I of the test, resistance to the lateral force was provided by a 3.66 m long load bearing RC rectangular wall, hereafter referred to as web wall. Thickness of the web wall was 200 mm at the first and seventh levels and 150 mm elsewhere. The web wall is directed East-West (loading direction) and provides support to seven 200 mm thick RC slabs spaced at 2.74 m. At the East and West directions of the web wall, two transverse walls were built to

provide lateral and torsional stability. The East wall, hereafter referred to as flange wall, was 4.87 m long, with a thickness of 200 mm at the first level and 150 mm elsewhere. The West wall was a precast, prestressed segmental wall with mortar bed joints. The footing of this wall enabled it to rock in the East-West direction, while the web and flange walls had fixed supports with footings that were tied down to the shake table. The test structure height, starting from the top of the foundation, was 19.2 m. The total mass excluding the foundation was 209.36 tons. Fig. 1 shows floor plans and perspective view of the test building slice, while the structural geometry and main dimensions are given in Fig. 2. Table. 1 gives the tributary seismic masses lumped at each floor.

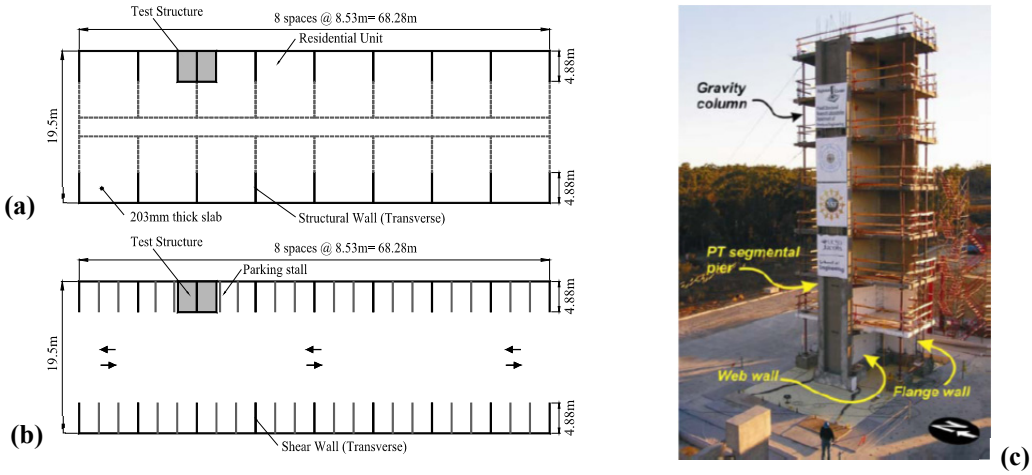

Figure 1. Plan of prototype building: (a) Residential floor plan; (b) Parking floor plan; and (c) Perspective view (Panagiotou et al., 2007)

Web and flange walls were linked with a 610 mm wide slab. The link slab had two, 140 mm deep by 51 mm wide, slots on both ends. These pin-pin connections had the capability of transferring in-plane diaphragm shear, moment and axial forces but had a reduced capacity to transfer out-of-plane actions during phase I of the test. The North and South ends of RC floor slabs were supported on four pin-ends gravity columns designed to carry axial tension and compression only. The columns were reinforced with Dywidag prestressing bars grouted inside 102 mm diameter, 8.6 mm thick high strength steel pipes to prevent buckling. Concrete with a target 27.6 MPa specified compressive strength and Grade 60 steel reinforcement were used in the test structure. The measured average concrete compressive strength at the day of the final test was 37.9 MPa, while the average measured reinforcing steel yield strength was 455 MPa. The footings under web and flange walls were longitudinally prestressed and designed to remain elastic during testing.

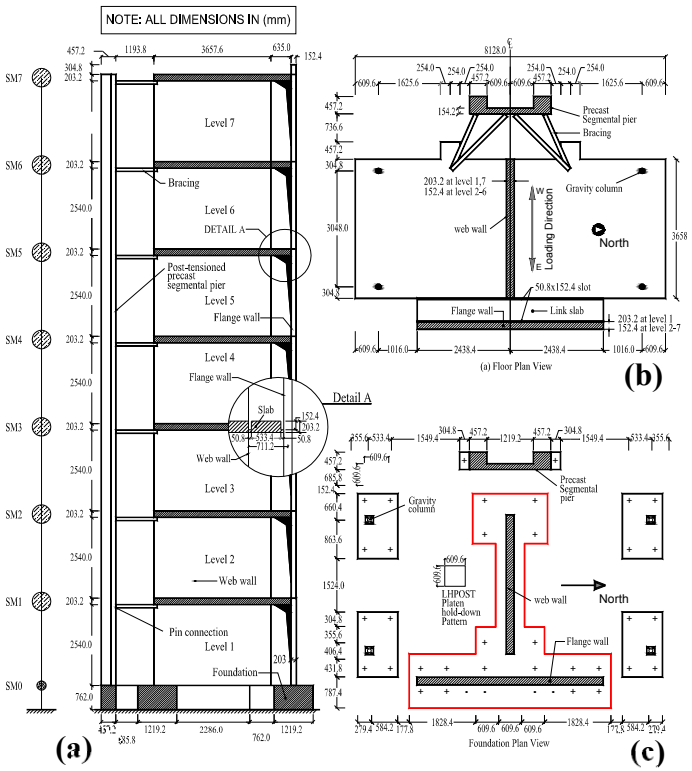

Figure 2. Test structure: (a) Elevation; (b) Floor plan view; and (c) Foundation plan view

2.2 INPUT GROUND MOTIONS

Phase I of the test program investigated the response of the cantilever web wall to four levels of excitations with increased intensities (EQ1-EQ4) representing four historical earthquakes recorded in Southern California. Prior to and between the earthquake tests, the structure was subjected to long-duration ambient vibration tests and long-duration low-amplitude white noise tests for system damage identification (Moaveni et al., 2010). The low intensity input motion EQ1 was the VNUY longitudinal component from the 1971 M_w 6.6 San Fernando earthquake. The two medium intensity input motions EQ2 and EQ3 were the VNUY transverse component record from the 1971 M_w 6.6 San Fernando earthquake and the WHOX longitudinal component from the 1994 M_w 6.7 Northridge earthquake respectively. The large intensity input motion EQ4 was the Sylmar Olive View Med 360^o component record from the 1994 M_w 6.7 Northridge earthquake. Fig. 3 shows the acceleration time-histories for the most intense 30 sec of each record as well as the acceleration and displacement response spectra of the four input motions. Table. 2 lists the peak recorded values of response parameters, while Table. 3 shows the measured fundamental periods of the test structure before the test and after applying each record.

Table 1. Seismic masses[#] (tons)

Mass Ref.	Slab	Web Wall	Flange Wall	Segmental Wall	Other	Total
SM0	0	2.30	3.20	2.00	0	7.50
SM1	17.20	4.00	5.60	4.00	0.78	31.58
SM2	15.90	3.40	5.00	4.00	0.78	29.08
SM3	15.90	3.40	5.00	4.00	0.78	29.08
SM4	15.90	3.40	5.00	4.00	0.78	29.08
SM5	15.90	3.40	5.00	4.00	0.78	29.08
SM6	15.90	4.00	5.00	4.10	0.78	29.78
SM7	15.90	2.30	3.10	2.10	0.78	24.18
Total	112.60	26.20	36.90	28.20	5.46	209.36

 # Foundation mass is excluded.

Table 2. Peak recorded values of relevant response parameters

Response Parameter	**EQ1**	**EQ2**	**EQ3**	**EQ4**
Roof relative lateral displacement (m)	0.05	0.14	0.16	0.38
Roof drift ratio (%)	0.28	0.75	0.83	2.06
Inter-story drift ratio*	0.35	0.89	1.03	2.36
Roof absolute acceleration (g)	0.43	0.61	0.75	1.10
Peak table acceleration (g)	0.15	0.27	0.35	0.91
System base shear (kN)[§]	425	628	704	1185
System base moment (kNm) [§]	5606	8093	8490	11839

***Overall stories.**

[§] Calculated as product of story mass with measured horizontal floor acceleration.

Table 3. Measured fundamental periods of the test structure

Stage	Measured Fundamental Period (s)
Before testing	0.51
After EQ1	0.65
After EQ2	0.82
After EQ3	0.88
After EQ4	1.16

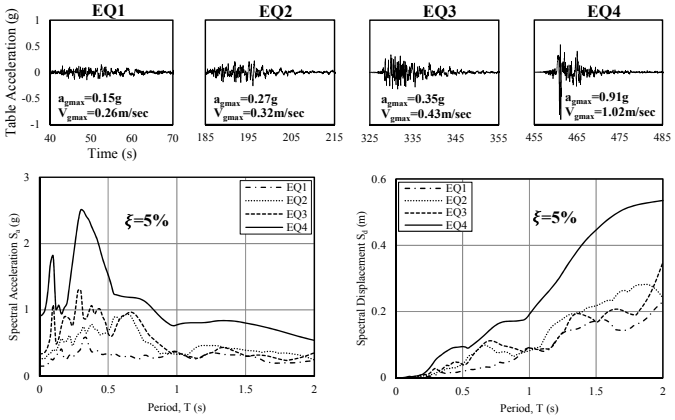

Figure 3. Phase-I time histories (most intense 30 sec) and response spectra of recorded table ground motions

2.3 ANALYTICAL MODELS AND RESULTS

Three analytical models are developed for this study. ZEUS-NL (Elnashai et al., 2012) is utilized to develop the first two: "Z-MODEL" and "IZ-MODEL"; while PERFORM-3D (CSI, 2011) is used to develop the third one: "P-MODEL". A brief description of the features of each model and the comparison between the predicted and measured results is given in the following sections. Fig. 4 shows schematic diagrams of the three models.

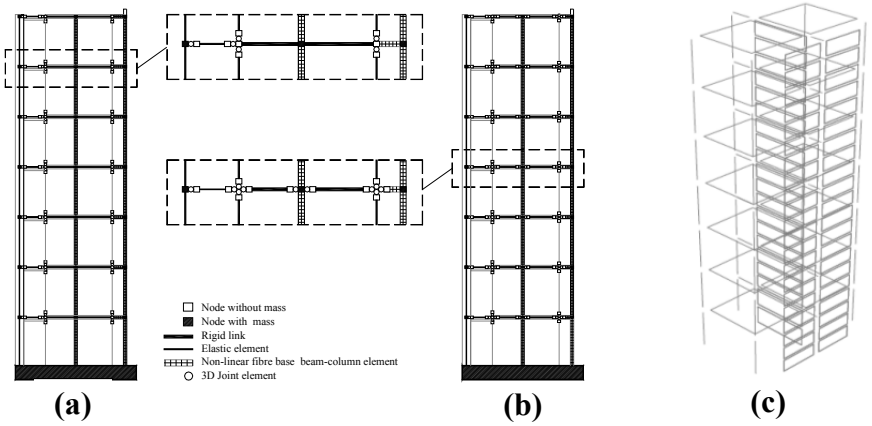

Figure 4. Schematic diagrams of developed models: (a) Z-MODEL; (b) IZ-MODEL; and (c) P-MODEL

2.3.1. Z-MODEL & IZ-MODEL

The Z-MODEL is a preliminary 2D (in the plane of excitations) analytical model for the test structure. The centreline model included the web wall, flange wall, gravity columns, prestressed segmental pier, link (slotted) slab and the braces connecting the segmental pier to the structure. Due to the lack of a special purpose shear wall element in the ZEUS-NL library, 2-noded fibre-based cubic elasto-plastic elements are used to model the response of web and flange walls. Elastic frame elements are used to model the prestressed segmental pier, the gravity columns and the braces. Rigid end offsets (rigid links) are used to connect the web wall centreline to the gravity column elements at both wall ends. A 3D joint element characterized by linear elastic behaviour is used to simulate the pin-pin connection of gravity columns, braces and the East-West hinge connection between the segmental prestressed pier and its footing. The seismic mass of the test structure (Table. 1) is lumped at floor levels to simplify the analytical model. The weight of the structure is also applied as nodal loads to account for gravity and P-Δ effects during NRHAs. Since the experimental results evidenced almost exclusively flexural behaviour at the base of the web wall, shear deformation is not accounted for in this study.

An improved Mander model (Martinez-Rueda and Elnashai, 1997) is used to calculate the properties of confined concrete which is assigned to the corresponding fibres in the web and flange walls cross-sections at the first story. The concrete in the upper stories had no confinement reinforcement and thus modeled using unconfined concrete fibres. Menegotto and Pinto (1973) uniaxial steel model is used to model steel reinforcing bars in the test structure. ZEUS-NL includes Rayleigh damping as an option to account for the effects of the viscous damping during dynamic analysis. However, the mathematical model of Rayleigh damping in this package is based on initial stiffness in calculating the damping matrix. Panagiotou and Restrepo (2006) used a damping ratio of 0.3% for the first longitudinal mode in simulating the test structure's response to earthquake input motions. The use of such a low damping ratio can account for the absence of nonstructural elements and also for the fact that flexural cracking was largely limited to the lower part of the structure as a consequence of the low ratio of longitudinal reinforcements that design approach of the building led to (i.e. displacement-based design). In the "Z-MODEL", a stiffness-proportional viscous damping corresponding to 0.5% damping ratio is used. The stiffness-proportional damping coefficient is calculated based on a weighted period; the mean cracked period of the first three translational modes in the direction of excitation weighted based on the mass participation factor from modal analysis and its corresponding spectral acceleration of the test structure. The mass-proportional damping coefficient is set to zero.

The input motions shown in Fig. 3 are applied to the base of the test structure model in the East-West direction parallel to the web wall. Using Newmark integration scheme, NRHA is conducted at a time step of 1/60 s. The four input motions, EQ1 to EQ4, are concatenated in order to account for the accumulated structural damage on the response of the test structure. Six seconds of zero base acceleration is added in between the earthquake records to allow the structure to come to rest prior to being subjected to the next record. The concatenated applied base motion record is 523 sec long in total.

The capability of the "Z-MODEL" in predicting the global response of the test structure during the most intense 30 sec of each of the four earthquake input motions is assessed by comparing the analytical results with measured data for top-floor relative displacement time-histories (Fig. 5), response envelopes of story displacement, ISD, story shear and story moment (Fig. 6). Fig. 5 shows that the model captures well all the significant peak relative displacements recorded during EQ1, EQ2 and EQ4, while the peak displacements on EQ3 are under predicted by as much as 25%. The discrepancies for the computed response of EQ3 have also been recorded in other studies (Kelly, 2007; Waugh and Sritharan, 2010). This can mainly be attributed to the similarity in earthquake intensity between EQ2 and EQ3 input motions. As a consequence of these two records having comparable intensities, the unloading and reloading paths of the material models rather than their envelopes have a big influence on the analytical response of EQ3. Accurate presentation of the unloading and reloading behaviours of the material models becomes more critical in predicting structural response when the earthquake motions do not move the structure significantly into a virgin territory. Such scenario is foreseen when predicting response to aftershocks following a structure's response to the main earthquake event. Fig. 6a shoes very good agreement between predicted and measured displacement envelopes at floor-levels (story displacement). As expected, the displacements of EQ3 are under predicted. The maximum roof drift ratios are found to be 0.30% for EQ1, 0.75% for EQ2 and 2.05% for EQ4, compared to their corresponding measured values of 0.28%, 0.75% and 2.06%, respectively. While for EQ3 response, the obtained and measured maximum roof drifts are 0.78% and 0.83%, respectively. An accurate prediction of ISDs is essential to predict damage to structural and non-structural elements in a building. ISD ratio is typically considered as a key parameter in defining performance limit states for seismic vulnerability assessment of high-rise buildings. As shown in Fig. 6b, the ISD envelopes are well predicted by the analysis for EQ1, EQ2 and EQ4, while for EQ3, it is within 30% of the experimental values for the reasons previously discussed.

Despite the very good agreement between predicted and measured response values of top displacement time-histories, story displacement envelopes and ISD envelopes discussed above, the "Z-MODEL" underestimates the story shear and consequently story moment envelopes of the test structure, especially when the structure behaves inelastically (Fig. 6c & d). The discrepancies between reported and analytical story shear and moment values can be attributed to the influence of the 3D interaction between gravity columns, floor slabs and the web wall to the overall lateral capacity of the test structure. The significant contribution of this interaction to the lateral force resistance of the test building was confirmed by Panagiotou and Restrepo (2006) using pushover analysis. The main reason for this influence is that, due to their interaction with the floor slab, the gravity columns developed significant axial strains during testing. Consequently, the columns near the tension side of the web wall were experiencing tensile forces and those closer to the compression side of the web wall were subjected to compression forces. Given the 3.05 m distance between the columns, the tension and compression forces enabled a large moment to be developed and effectively increased the lateral force resistance of the test structure.

To address this issue, the "IZ-MODEL" is developed to introduce the 3D slab-columns-web interaction effect. In the "IZ-MODEL", 3D joint elements are introduced at both ends of the rigid link that connects the web wall centreline to the gravity columns at each floor level (Fig. 4b). A bilinear asymmetric moment-curvature relation is assigned to those elements to simulate the out-of-plane flexural rigidity of the slab. Fig. 7 shows the story shear and moment envelopes predicted using the "IZ-MODEL" for EQ1 to EQ4, where a significant improvement can be seen. This exercise highlights the importance of taking into account the 3D interaction effect of all structural members in a building, including members which are not part of the lateral force resisting system such as gravity columns and diaphragm slabs, to accurately predict seismic response.

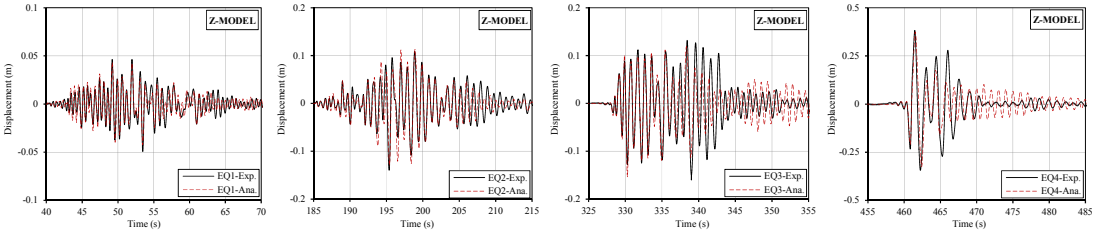

Figure 5. Z-MODEL: Measured versus computed top relative displacement during the Four Input Motions

For a more accurate assessment of the capability of "IZ-MODEL" to capture the damage evolution of the test structure during the four input motions with increasing intensities, the frequency spectrum of the top relative displacement time-histories for EQ1 to EQ4 is plotted in Fig. 8 using the Fast Fourier Transform (FFT) method. It is worth noting that the measured fundamental frequency of the test structure changed from 1.96 Hz before testing to 0.86 Hz at the end of EQ4, with corresponding fundamental periods of 0.51 s and 1.16 s, respectively. Despite the significant lengthening of the fundamental period of the test structure by more than double, the "IZ-MODEL" was able to track this damage progression with very high accuracy. Another measure of the capability of the analytical model is the determination of local damage. Fig. 9 shows the envelope of tensile strains in an outer reinforcing bar, marked as ST2 in the testing, along the height of the first level for EQ4 input motion. Computed strains can be sensitive to the element mesh, especially at zones of concentrated plasticity (plastic hinge zone). To investigate the influence of meshing size on the computed stains, the web wall member in the first level of the building is modeled using four different meshes: one element-mesh (1E); two elements-mesh (2E); three elements-mesh (3E); and six elements-mesh (6E). The results presented in Fig. 9 show that the "IZ-MODEL" with 2E-mesh predicted the tensile strain envelops of ST2 reinforcing bar with high accuracy. This confirms the capability of the implemented material models to estimate the force-deformation hysteresis and consequently the strain envelop. It is worth noting that with the 2E-mesh, the length of each element (1321 mm) is close to the expected plastic hinge length developing at the wall base (0.5 times the flexural depth of the web wall = 1830 mm) as proposed by FEMA (2000).

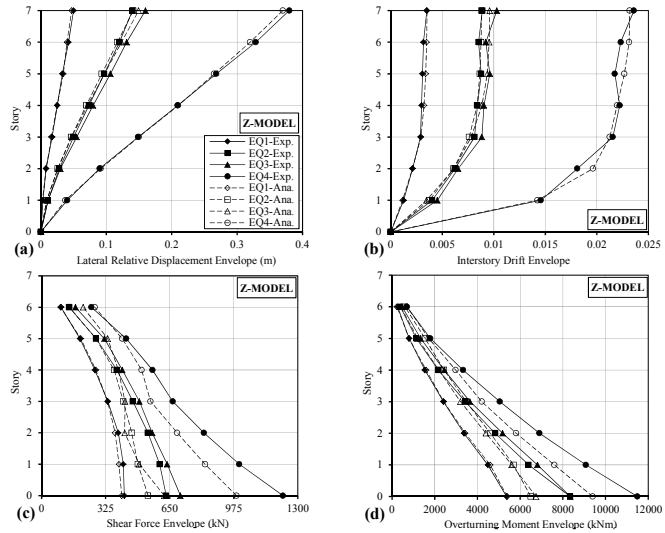

Figure 6. Z-MODEL: Measured versus computed envelopes: (a) Relative displacement; (b) Inter-story drift; (c) Story shear; and (d) Story moment

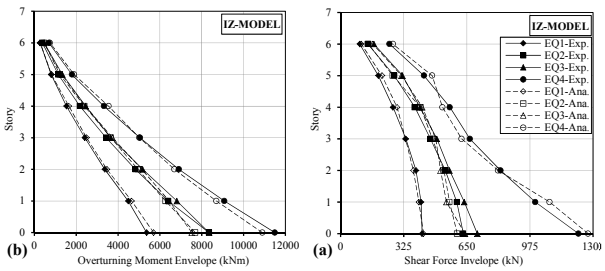

Figure 7. IZ-MODEL: Reported versus computed envelopes: (a) Story shear; and (b) Story moment

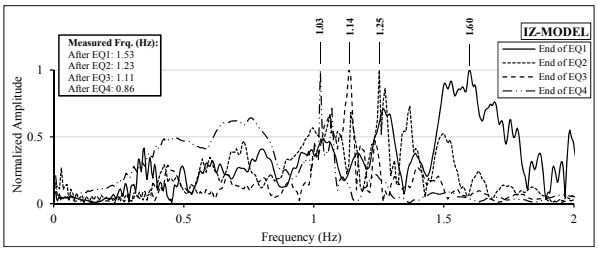

Figure 8. IZ-MODEL: Evolution of frequency spectrum during the for the four input motions

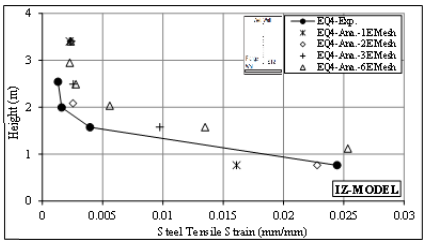

Figure 9. IZ-MODEL: Tensile strain of ST2 reinforcing bar over the height of first level for EQ4

2.3.2. P-MODEL

The "P-MODEL" is developed using PERFORM-3D (CSI, 2011) analytical tool to evaluate the program's capability in predicting the response over the four earthquake records for the test structure. To model the web and flange walls, a 4-noded fibre-based shear wall element is used with nonlinear vertical fibres to represent the behaviour of concrete and reinforcing steel. Based on the outcome of the element mesh sensitivity study conducted with the "IZ-MODEL" in Section 2.3.1, web and flange walls are represented with two elements in the first level. The link slab is modeled using 2-noded fibre-based frame element. An elastic frame element with specified cross-section properties is used to model the prestressed segmental pier, while elastic bar element is utilized to model the pin-pin end braces and gravity columns. The cross-section properties of these members are calculated based on the reported section geometry and material properties. Finally, an elastic 4-noded slab element is used to represent the floor slabs. For the sake of comparison, the modelling of the seismic mass of the test structure followed the principles used in the "Z-MODEL" and "IZ-MODEL". Despite the option available in PERFORM-3D to account for the shear deformation in a shear wall element by defining the inelastic shear stress-strain material relation, shear deformation is not accounted for to enable a direct comparison with their counterparts predicted by the "IZ-MODEL". Trilinear stress-strain relationships are used to model the concrete and reinforcing steel materials with similar material properties that are used in the ZEUS-NL models. For the reinforcing steel material model, the cyclic degradation parameters are defined following the adjustments described by Orakcal and Wallace (2006). A linear stress-strain relation is used to model the materials of the prestressed segmental pier, floor slabs, braces and gravity columns. For consistency, Rayleigh damping is used in the "P-MODEL" with the same parameters assumed in the 'Z-MODEL" and "IZ-MODEL".

Following the same sequence used in Section 2.3.1, Figs. 10, 11, 12 and 13 show predicted versus measured top-floor relative displacement time-histories, response envelopes, frequency spectrums and ST2 steel bar tensile strain, respectively. A very good agreement can be seen for all predicted responses. Again, for the same reasons discussed in the previous section, predicted responses for the test structure under EQ3 have some discrepancies when compared with measured values.

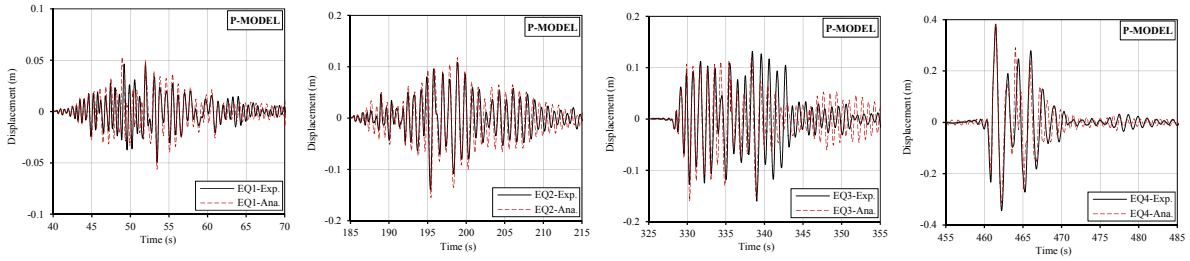

Figure 10. P-MODEL: Measured versus computed top relative displacement during the four input motions

While the data measured from the shake table test confirmed the accuracy of the investigated analytical models in predicting global responses and local damages, some limitations also became apparent. The study reveals the ability of fibre-based 4-noded wall/shell element to account for 3D effects of deformation compatibility between lateral and gravity-force-resisting systems. The study also addresses the sensitivity of attained results to the stiffnesses of the rigid links required to connect the shear walls to neighbouring elements when a 2-noded beam-column line element modelling approach is used.

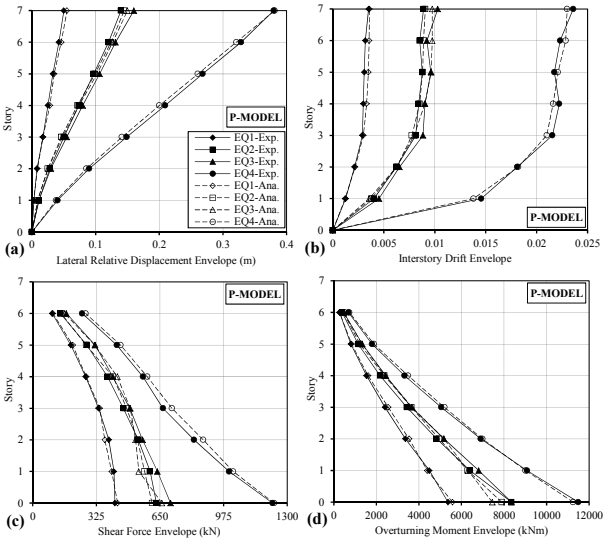

Figure 11. P-MODEL: Measured versus computed envelopes: (a) Relative displacement; (b) Inter-story drift; (c) Story shear; and (d) Story moment

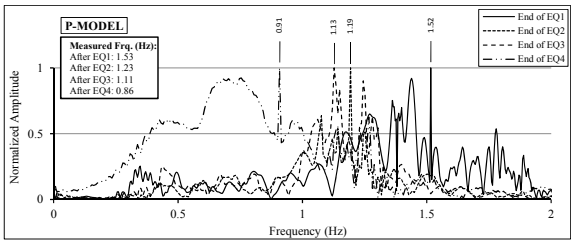

Figure 12. P-MODEL: Evolution of frequency spectrum during the four Input Motions

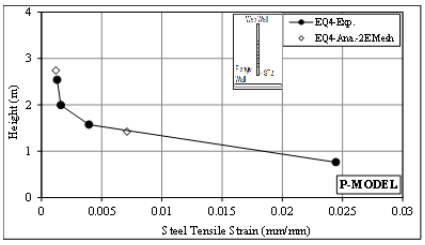

Figure 13. P-MODEL: Tensile strain of ST2 reinforcing bar over the height of first level for EQ4

Based on the modelling verification results presented in this section, PERFORM-3D was adopted to model the 30-story RC wall building used as a sample structure to illustrate the additional steps required to develop ASFRs.

3. SAMPLE STRUCTURE

A 30-story RC wall building (2 basement + ground floor + 27 typical floors) is used in this paper to illustrate the additional steps required to develop ASFRs. The building is located in Dubai (UAE). The seismic design loads are calculated as per ASCE7 (2010) and IBC (2012) with the mapped acceleration parameters recommended for Dubai based on previous PSHA studies. Structural elements are proportioned and detailed using the load combinations and design provisions of ACI318 (2011). The concrete strength used for the structural elements ranges between 40-50 MPa with Grade 60 reinforcing bars having diameters of 10-32 mm. Fig. 14 shows the typical layout, 3D design model and PERFORM-3D nonlinear model of the sample structure.

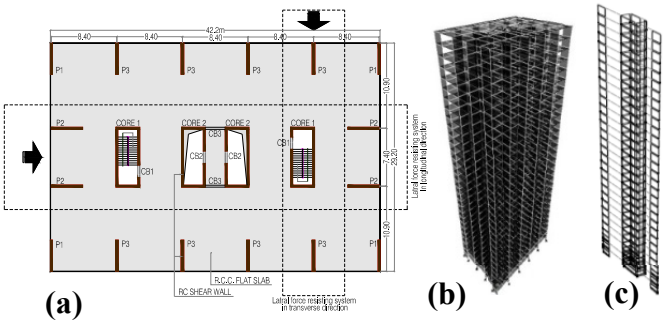

Figure 14. 30-story bearing wall sample building: (a) Typical layout; (b) 3D design model; and (c) PERFORM-3D model

4. NONLINEAR MODEL

3D slice in the transverse direction (Fig. 14c) is modelled using PERFORM-3D. The associated cracked period summary is provided in Table. 4. In this model, fibre-based elements are utilized to model RC slab, piers and core, while coupling beams are modeled using elastic beam element with nonlinear displacement shear hinge. The concept described in Section 2.3.2 is used to model viscous damping and the structural materials. Shear deformation is not accounted for.

5. UNCERTAINTY MODELLING

The vulnerability analysis is probabilistic in nature due to the uncertainties of its demand and capacity ingredients. Previous studies had concluded that the uncertainties in input ground motions are more significant compared to those due to structural properties (Porter et al., 2002). In the present study, only the uncertainties in input ground motions are considered. Uncertainties related to material properties, structural modelling and analysis method are assumed deterministic. To perform NRHAs for the sample structure, two sets of natural earthquakes with 20 records each are selected from both the European Strong-motion and PEER Databases. The records are selected based on magnitude, *M*, distance to source, *R*, site soil condition, *S* and ratio of peak acceleration-to-velocity, *a/v*, to represent the two earthquake scenarios in which the Dubai region is vulnerable to: (i) strong distant long-period events; and (ii) moderate near-field short-period events. Due to space limitations, only the IDAs and ASFRs results based on the long-period set of records are presented. Table. 5 lists the 20 long-period records, while Fig. 15 shows the 5% damped response spectra for the selected input ground motions

anchored at the weighted period (2.54 s) alongside the IBC design spectra of the study site for soil classes C and D.

Table 4. Cracked periods for the first three vibration modes in the transverse direction

Vibration Mode in Transverse Direction	Period (s)	Mass participation (%)
1	4.5	66
2	0.96	18
3	0.39	7

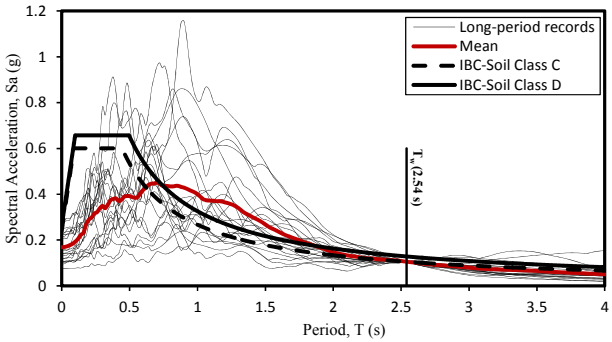

Figure 15. 5% Damped response spectra for the 20 long-period records anchored at the weighted period of the sample structure

Table 5. List of the 20 long-period earthquake ground motion records

Ref	Earthquake	Station	Comp.	Date	M_w	Soil# Class	Dist. (km)	Duration (sec)	PGA (m/s^2)	(a/v)* g/ms^{-1}	(a/v) Class
R1	Bucharest	Building Res. Inst.	EW	04-03-1977	53	Stiff	161	18	1.73	0.60	
R2	Chi-Chi	CWB-ILA013	EW	20-09-1999	7.62	V. dense	135	117	1.36	0.52	
R3	Loma Prieta	Emeryville	260	18-10-1989	93	V. dense	96.5	39	2.45	0.57	
R4	Loma Prieta	Golden Gate Bridge	270	18-10-1989	93	V. dense	100	38	2.29	0.61	
R5	Hector Mine	Indio-Coachella C.	0	16-10-1999	13	Stiff	99	60	0.90	0.70	
R6	Izmit	Ambarli-Termik	EW	17-08-1999	64	Stiff	113	150	1.80	0.60	
R7	Izmit	Istanbul-Zeytinburnu	NS	17-08-1999	64	Stiff	96	129	1.08	0.77	
R8	Kocaeli	Bursa Tofas	E	17-08-1999	51	Stiff	95	139	1.06	0.49	
R9	Kocaeli	Hava Alani	90	17-08-1999	51	V. dense	102	106	0.92	0.46	low
R10	Loma Prieta	Alameda Naval ASH	270	18-10-1989	93	Stiff	91	29	2.39	0.73	
R11	Loma Prieta	Berkeley LBL	90	18-10-1989	93	V. dense	98	39	1.15	0.65	
R12	Loma Prieta	Oakland-OHW	0	18-10-1989	93	Stiff	94	40	2.75	0.67	
R13	Manjil	Abhar	N57E	20-06-1990	42	Stiff	91	29	1.30	0.62	
R14	Manjil	Tonekabun	N132	20-06-1990	42	V. dense	131	40	1.22	0.76	
R15	Chi-Chi	TAP005	E	20-09-1999	62	Stiff	156	134	1.34	0.49	
R16	Chi-Chi	TAP010	E	20-09-1999	62	Stiff	151	144	1.19	0.50	
R17	Chi-Chi	TAP021	E	20-09-1999	62	Stiff	151	125	1.15	0.47	
R18	Chi-Chi	TAP032	N	20-09-1999	7.62	V. dense	144	90	1.13	0.64	
R19	Chi-Chi	TAP090	E	20-09-1999	7.62	Stiff	156	125	1.28	0.41	
R20	Chi-Chi	TAP095	N	20-09-1999	62	Stiff	158	123	0.96	0.52	

#Soil Class: V.dense (V_{s30} = 360-760 m/s), Stiff (V_{s30} = 180-360 m/s)
*(a/v) Classification: Low < 0.8, High > 1.2

6. DERIVATION OF FRAGILITY RELATIONS

The seismic demand of the sample structure is obtained from NRHAs using the input ground motions described in Section 5 with each record scaled to multiple levels of intensity (IDAs). To determine the distribution of the statistics along the horizontal axis of the IDA and fragility plots, an intensity measure has to be selected. Several IMs were proposed by researchers in previous studies such as Peak Ground Acceleration (PGA), Spectral Displacement (SD) and Spectral Acceleration (SA). In the present study, spectral acceleration at the weighted period of the structure is used, $S_a(T_w, 5\%)$. To ensure that each record is properly scaled to cover the entire range of structural response and yet minimizing the number of required runs, the *hunt & fill* scaling algorithm by Vamvatsikos and Cornell (2002) is used. ISD is selected as DM because it can be related to the performance levels of RC buildings in various guidelines and previous studies (ASCE/SEI 41, 2007; Ghobarah 2004; Ji et al, 2009). The expression proposed by Wen et al. (2004) to derive the fragility relations is utilized in this study. In this expression, a value of 0.2 is assigned to the factor associated to the uncertainty in analytical modelling. This decision is made based on the assumption that the response estimates of the sample structure using the verified modelling approach described in Section 2.3.2 are within 30% of the actual values with 90% confidence (Wen et al., 2003).

Following the approach of ASCE/SEI 41 (2007), three limit states are considered in the present work for the derivation of fragility relations, namely (i) IO; (ii) LS; and (iii) CP. In the literature, different values of ISD are assigned to define performance levels of RC ductile wall structures. Table. 6 lists three examples of different ISD values adopted by various seismic guidelines and previous studies. In the current work, the fragility relations are developed for upper and lower bands of the range of ISD values given in Table. 6 to illustrate the significance of ISD selected values in shaping the fragility curves and evaluating the damage state probabilities. The considered ranges for ISD values are 0.2-0.5, 0.52-1.5 and 1.1-2.5 for IO, LS and CP limit states, respectively. Fig. 16 presents IDA results (300 ISD-S_a points) obtained for the sample building from the ground motion set listed in Table. 5 with the power law used to derive the fragility relations. Fig. 17 shows the IDA curves for the 20 records with 16%, 50% and 84% fractiles, while Fig. 18 presents the fragility relations for the three adopted limit states with the lower and upper bands of the considered ISDs crossed by two lines representing the design spectral acceleration values for Dubai soil types C and D. In Fig. 18c, the fragility of the sample building is presented in terms of damage probabilities of each PLS at the design spectral acceleration. the significant differences in damage probabilities observed in Fig. 18 for each PLS when lower and upper bands of ISDs are used stresses the sensitivity of ASFRs to the DM values used to define the PLSs.

Table 6. Definition of limit states with ISD for RC ductile wall structures by various references

Reference	Limit States		
	IO	LS	CP
Chobarah (2004)	0.4	1.5	2.5
ASCE/SEI 41 (2007)	0.5	1.0	2.0
Ji et al. (2009)	0.2	0.5	1.1

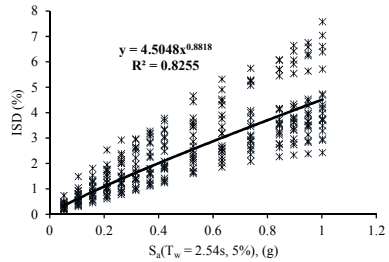

Figure 16. IDA results from 20 long-period records

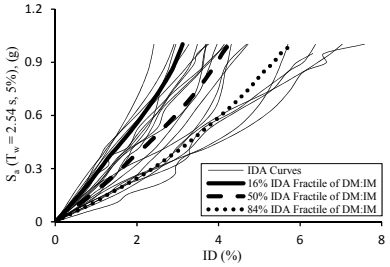

Figure 17. IDA curves from 20 long-period records

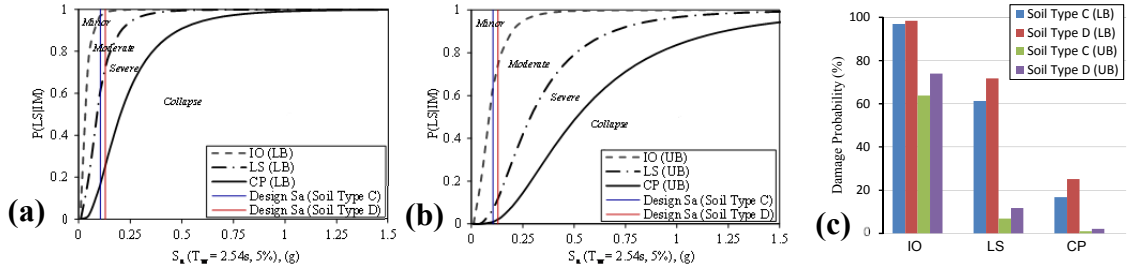

Figure 18. Fragility relations of the sample building obtained from IDAs using 20 long-period earthquake ground motion records: (a) Lower band (LB); (b) Upper band (UB); and (c) Damage probability

7. SUMMARY AND CONCLUSIONS

A framework for developing reliable analytical seismic fragility relations for code-compliant, RC high-rise wall structures was presented in this paper. A multi-level verification scheme was conducted to investigate different approaches and parameters of nonlinear analytical modelling of RC buildings with slender shear walls and cores. The seven-story wall building slice tested in full scale on LHPOST at UCSD was used in the verification scheme by comparing its results with three different modelling techniques. As an example, incremental dynamic analyses with improved scalar intensity measure was used to develop the fragility relations for a 30-story RC wall building located in the Emirate of Dubai, a region that is taken as case study in the current work. The selection and scaling of two sets of natural earthquake records (40 records in total) representing strong distant and moderate near-field earthquake scenarios anticipated in the study region were briefly discussed. The effect of ISD values used to

define performance limit states on the derived fragility relations were investigated by applying upper and lower bands selected from seismic guidelines and previous studies. The paper reveals the superior performance of fibre-based 4-noded wall/shell element modelling approach in accounting for 3D effects of deformation compatibility between lateral and gravity-force-resisting systems. It also emphasizes the sensitivity of ASFRs to the DM values used to define the PLSs. While the verifications with full-scale shake table test results confirmed the excellent accuracy of the developed analytical models in predicting seismic response, it is recommended to investigate the implications of shear deformation in RC wall components and the Soil-Foundation-Structure-Interaction (SFSI) to arrive at a more reliable ASFRs framework for high-rise buildings. Since nonlinear modelling of structures is the core to analytical-based seismic fragility relations, the verified approaches and calibrated modelling parameters presented in this paper are essential to achieve a reliable outcome.

REFERENCES

ACI 318-11 (2011) Building Code Requirements for Structural Concrete and Commentary, American Concrete Institute Committee 318, Farmington Hills, MI

ASCE/SEI 7 (2010) Minimum Design Loads for Buildings and Other Structures, ASCE Standard ASCE/SEI 7-10, American Society of Civil Engineers, Reston, VA

ASCE/SEI 41(2007) Seismic Rehabilitation of Existing Buildings, ASCE Standard ASCE/SEI 41-6, American Society of Civil Engineers, Reston, VA

CSI (2011) Computer and Structures Inc. Perform-3D V5: Nonlinear Analysis and Performance Assessment for 3D Structures, 1995 University Avenue, Berkeley, CA.

Elnashai AS, Papanikolaou V, Lee D (2012) Zeus-NL – A System for Inelastic Analysis of Structures-User Manual, Mid-America Earthquake Centre, Uni. Of Illinois at Urbana-Champaign, Urbana, IL

FEMA356 (2000) Prestandard Commentary for the Seismic Rehabilitation of Buildings, Federal Emergency Management Agency, Washington, DC

Gobarah A (2004) "On Drift Limits Associated with Different Damage Levels", *International Workshop on Performance-based Seismic Design*, Dept. of Civil Engineering, McMaster Univ., Canada

IBC, International Building Council (2012) International Building Code, Falls Church, VA

Ji J, Elnashai AS, Kuchma DA (2009) "Seismic Fragility Relationships of Reinforced Concrete High-rise Buildings:, The Structural Design of Tall and Special Buildings, 18(3): 259-277

Kelly T (2007) "A Blind Prediction Test of Nonlinear Analysis Procedures for Reinforced Concrete Shear Walls", *Bulletin of the New Zealand Society for Earthquake Engineering*, 40(3): 142-159

Martínez-Rueda JE and Elnashai AS (1997) "Confined Concrete Model under Cyclic Load", *Materials and Structures*, 30(3):139-147

Menegotto M and Pinto P (1973) "Method of Analysis for Cyclically Loaded Reinforced Concrete Plane Frames Including Changes in Geometry and Non-elastic Behaviour of Elements Under Combined Normal Force and Bending", *IABSE Symposium on the Resistance and Ultimate Deformability of Structures Acted on by Well-Defined Repeated Loads*, Lisbon.

Moaveni B, He X, Conte JP (2010) Damage Identification Study of a Seven-story Full-scale Building Slice Tested on the UCSD-NEES Shake Table, Structural Safety, 32(5), 347-356

Mwafy A (2010) "Analytically Derived Fragility Relationships for the modern High-rise Buildings in UAE", *The Structural Design of Tall and Special Buildings*, 21(11): 824-843

Orakcal K and Wallace JW (2006) "Flexural Modelling of Reinforced Concrete Walls – Experimental Verification." *ACI Structural Journal*, 103(2): 196-206.

Panagiotou M, Restrepo J, Conte JP (2007) Shake table test of a 7 story full scale reinforced concrete structural wall building slice phase I: Rectangular Wall Section, Report No. SSRP: 07-07, Department of Structural Engineering, Univ. of California, San Diego, CA.

Panagiotou M and Restrepo J (2006) "Model Calibration for the UCSD 7-Story Building Slice", *NEES-UCSD Workshop on the Analytical Model of Reinforced Concrete Walls*, San Diego, CA.

Porter KA, Beck JL, Shaikhutdinov RV (2002) "Sensitivity of Building Loss Estimates to Major Uncertain Variables", *Earthquake Spectra*, 18(4): 719-743

Vamvatsikos D and Cornell CA (2002) "Incremental Dynamic Analysis", *Earthquake Engineering & Structural Dynamics*, 31(3): 491-514

Waugh JD and Sritharan S (2010) "Lessons Learned from Seismic Analysis of A Seven-story Concrete Test Building" *Journal of Earthquake Engineering*, 14(3): 448-469

Wen YK, Ellingwood BR, Veneziano D, Bracci J (2004) Vulnerability Function Framework for Consequence-based Engineering, DS-4 Report, Mid-America Earthquake Centre, Uni. Of Illinois at Urbana-Champaign, Urbana, IL

Wen YK, Ellingwood BR, Veneziano D, Bracci J (2003) Uncertainty Modelling in Earthquake Engineering, FD2 Report, Mid-America Earthquake Centre, Uni. Of Illinois at Urbana-Champaign, Urbana, IL